

**THE ROVIBRATIONAL DEPENDENCE OF THE  $^{14}\text{N}$  NUCLEAR QUADRUPOLE COUPLING CONSTANTS IN THE  $X^2\Sigma^+$  AND  $B^2\Sigma^+$  STATES OF CN FROM THE MULTIREFERENCE CI APPROACH**Rudolf POLÁK<sup>a,\*</sup> and Jiří FIŠER<sup>b</sup><sup>a</sup> J. Heyrovský Institute of Physical Chemistry, Academy of Sciences of the Czech Republic, 182 23 Prague 8, Czech Republic; e-mail: rudolf.polak@jh-inst.cas.cz<sup>b</sup> Department of Physical and Macromolecular Chemistry, Faculty of Science, Charles University, 128 40 Prague 2, Czech Republic; e-mail: fiser@natur.cuni.cz

Received August 6, 2002

Accepted October 22, 2002

*Dedicated to Professors Petr Čársky, Ivan Hubač and Miroslav Urban on the occasion of their 60th birthdays.*

In using several augmented correlation-consistent basis sets and reference configuration spaces, the  $^{14}\text{N}$  quadrupole coupling constants (QCCs) of rovibrational levels of the  $X^2\Sigma^+$  and  $B^2\Sigma^+$  states of the CN radical are computed from internally contracted multireference configuration interaction wave functions. To examine the overall quality of the correlated wave functions used for computing the expectation values of the electric field gradient (EFG) tensor at the N nucleus, electric dipole moments are calculated and spectroscopic constants are derived from corresponding potential energy curves. The adequacy of the expectation value approach to the evaluation of the EFG and dipole moment is discussed. The calculated vibrational dependence of the  $^{14}\text{N}$  QCC compares reasonably with the available experimental data.

**Keywords:** CN radical; Electric field gradient; Nuclear quadrupole coupling constant of  $^{14}\text{N}$ ; Electric dipole moment; Spectroscopic constant; Vibrational spectroscopy.

The CN radical ranks among the most carefully studied species in molecular spectroscopy. Much of the impetus behind the investigation of the microwave spectrum of CN stems from the desire to identify and analyze microwave emission signals emanating from extraterrestrial sources<sup>1,2</sup>, which is reflected by the fact that many important contributions to the clarification of the problem have appeared in astrophysical journals. The first astronomical microwave observations of CN have been made by Jefferts *et al.*<sup>3</sup> in the Orion-A molecule cloud using a radio telescope, which only few years later was followed by the astronomical determination of the CN ( $X^2\Sigma^+$ ) hyperfine

structure in the free molecule<sup>4</sup>. The first laboratory microwave spectrum of CN in the  $v = 0, 1$  vibrational states of the electronic ground state, yielding the hyperfine coupling constants was reported by Dixon and Woods<sup>5</sup>. Interestingly enough, however, hyperfine structure laboratory measurements on excited electronic states of CN, particularly the  $B^2\Sigma^+$  molecular state<sup>6,7</sup>, were performed earlier than on the  $X^2\Sigma^+$  state. A new series of rotational parameters, including the  $^{14}\text{N}$  quadrupole coupling constants for the  $v = 0, 1$  states in the  $X$  state, was published by Klisch *et al.*<sup>8</sup>

CN is also a favorite probe species for open-shell systems in quantum chemical treatments<sup>9-12</sup>, since the quantum chemical calculation of electronic properties of CN presents a relatively "difficult case"<sup>10,12</sup>. Because of the important role of this species in combustion and spectroscopical processes, much effort has been devoted to establish reliable theoretical predictions on various physical properties, such as energy levels<sup>13-16</sup>, dipole moments<sup>12,17-19</sup>, transition probabilities<sup>13,19</sup>, spectroscopic<sup>14,19,20</sup> and hyperfine structure constants<sup>17,21</sup>, *etc.* Due to the unpaired electron in the  $^2\Sigma^+$  state, the hyperfine structure of CN arises primarily from the interaction of the  $^{14}\text{N}$  magnetic moment with the electron-spin magnetic moment<sup>22</sup>. A smaller contribution, characterized by the magnitude of the nuclear quadrupole coupling constant<sup>22</sup> (NQCC), comes from the interaction of the  $^{14}\text{N}$  electric quadrupole moment with the electric field produced by the electric charge of the C nucleus and molecular electrons. The sensitiveness of the NQCC to the electron environment of a quadrupolar nucleus can be used to investigate<sup>22-24</sup> the electronic structure and character of bonding in a molecule. The first attempts at interpreting the NQCC in CN took already place in the mid-sixties<sup>7,25</sup>. Cummins *et al.*<sup>26</sup> applied configuration interaction and coupled-pair functional methods to the calculation of the electric field gradients (EFGs) at the nitrogen nucleus in a number of molecules (including CN) in their ground electronic and vibrational states. However, advances in experimental methods make it now possible to obtain accurate information about NQCCs in various rovibronic states<sup>27-29</sup>.

Therefore, on grounds of our previous computational experience<sup>30-32</sup> with nuclear quadrupole interactions in various rovibrational levels of selected diatomic first-row hydrides and  $\text{CN}^+$  and  $\text{CN}^-$  ions, we decided to investigate the rovibrational dependence of the NQCCs for the CN radical in its two lowest  $^2\Sigma^+$  electronic states. An insight into the overall quality of the multireference configuration interaction (MRCI) wave functions used in the calculations was sought in determining electric dipole moments and deriving spectroscopic data from potential energy curves, and comparing them with available experimental and theoretical data. Since the MRCI wave

functions were utilized for computing EFG and dipole moment expectation values, possible non-Hellmann–Feynman corrections<sup>26</sup> to the results were discussed.

## THEORETICAL

The procedure employed in the calculations of electric properties for given electronic, vibration and rotation quantum states of a diatomic molecule consists of two steps<sup>33,34</sup> which are derived from the Born–Oppenheimer approximation scheme. The first step, related to the motion of electrons, produces electronic wave functions, corresponding energy eigenvalues,  $E_j$ , and other studied physical quantities as functions of the internuclear separation  $R$ . The second step comprises rovibrational averaging of the property curves for the given electronic state  $j$  by using rovibrational wave functions associated with the potential energy curve (PEC)  $E_j(R)$ .

The electronic structure calculations were performed by using the internally contracted multireference configuration interaction (icMRCI) method of Werner and Knowles<sup>35,36</sup>, as implemented in the MOLPRO (version 2000.1) suite of programs<sup>37</sup>, which offers an efficient and balanced way of treating multiconfiguration effects in the whole region of interatomic separations for the ground and excited electronic states. The orbitals for the CI calculations of the two lowest  $^2\Sigma^+$  electronic states are derived from a multi-configuration self-consistent field (MCSCF) solution, obtained either in two-state-averaged (2-S) complete-active-space SCF (CASSCF) calculations<sup>38,39</sup> or in single-state (1-S) CASSCF calculations, if applied only to the treatment of the electronic ground state (GS). For the description of the thirteen-electron system, active spaces (ASs) of various dimensions were used, ranging from eight valence orbitals  $3\sigma - 6\sigma, 1\pi, 2\pi$  to eleven orbitals, *i.e.*,  $1\sigma - 7\sigma, 1\pi, 2\pi$  and  $3\sigma - 7\sigma, 1\pi - 3\pi$ , denoted by (422)  $\equiv (4 \times a_1, 2 \times b_1, 2 \times b_2, 0 \times a_2)$ , (5+2,22)  $\equiv ([5+2] \times a_1, 2 \times b_1, 2 \times b_2, 0 \times a_2)$  and (533)  $\equiv (5 \times a_1, 3 \times b_1, 3 \times b_2, 0 \times a_2)$ , respectively, in  $C_{2v}$  symmetry. The inclusion of the  $1\sigma$  and  $2\sigma$  orbitals into the AS in some cases, visualized by “+2” in the notation, allowed to provide estimates of the core correlation contributions to the electric properties.

Three augmented correlation-consistent spdffg basis sets of Dunning and coworkers<sup>40–42</sup>, denoted by aug-cc-pVQZ, aug-cc-pV5Z and aug-cc-pCV5Z have been used. Note that the basis sets had to be restricted to the subset of spdffg functions for which the calculation of the EFG integrals is implemented in MOLPRO. These sets were further extended by one diffuse *s* function on each atom ( $\zeta_s(\text{C}) = 0.015$ ,  $\zeta_s(\text{N}) = 0.018$ ), leading to the final AO basis sets denoted by aVQZ, aV5Z and aCV5Z, respectively. The diffuse

functions appeared to be useful in earlier calculations<sup>32</sup> on  $\text{CN}^+$  and  $\text{CN}^-$ , and also in the case of CN the diffuse functions are expected to improve the representation<sup>12</sup> of the outer regions of the wave functions, mainly those of the excited electronic states.

The basic spectroscopic constants derived from the PECs were obtained using the subroutine VIBROT, a component of the MOLCAS-4 suite of *ab initio* programs<sup>43</sup>. The effect of higher excitations on the PECs and corresponding spectroscopic constants has been assessed by the multireference analog of the Davidson correction<sup>44,45</sup>, denoted by icMRCI+Q. The wave functions of the two lowest  $^2\Sigma^+$  electronic states of CN were used for computing expectation values (EV) of the electric dipole moment  $\mu(\mathbf{R})$  and the  $zz$ -component of the Born–Oppenheimer electric field gradient (EFG) tensor at nucleus A,  $q^{\text{A}}(\mathbf{R})$ , as functions of  $\mathbf{R}$ , with  $z$  lying in the molecular axis. The energy derivative (ED) method based on the finite field approximation<sup>26,46,47</sup> (with perturbing electric field of  $\pm 0.001$  a.u.), implemented in MOLPRO for the calculation of dipole moments, was utilized for controlling some results.

In the second step, the EFGs  $q_{j,vN}^{\text{A}}$  were calculated as expectation values of  $q^{\text{A}}(\mathbf{R})$  over the radial parts of rovibrational wave functions  $\chi_{j,vN}(\mathbf{R})$ , where the compound label of the symbols denotes the electronic ( $j$ ), vibrational ( $v$ ) and end-over-end rotational ( $N$ ) quantum numbers of the molecular state considered. These radial functions were obtained by solving the one-dimensional Schrödinger equation for nuclear motion using the Cooley–Numerov technique<sup>48</sup> by taking the pertinent potentials as cubic taut spline fits<sup>49</sup> to the potential energies. The rovibrationally dependent NQCCs are then

$$X_{j,vN}^{\text{A}} = eQq_{j,vN}^{\text{A}} / h, \quad (1)$$

where  $Q$  is the effective nuclear electric quadrupole moment of the nucleus A, e.g.,  $Q(^{14}\text{N}) = 0.02044 \text{ b}^{50}$ . Particularly, the  $^{14}\text{N}$  QCC value in MHz is obtained by multiplying the EFG/a.u. by 4.802678. In a similar way, the dipole moments for various vibrational states were determined by averaging the  $\mu(\mathbf{R})$  curve over the radial parts of the corresponding vibrational wave functions.

## RESULTS AND DISCUSSION

The typical behavior of the  $R$ - and  $v$ -dependences of the studied physical properties related to the  $X^2\Sigma^+$  and  $B^2\Sigma^+$  states of CN is characterized in graphs comprising Figs 1 and 2. Other types of calculations, using different AO basis sets and/or active orbital spaces, yield comparable results. In Fig. 1a the MCSCF and icMRCI  $q^{\text{N}}(R)$  curves for both electronic states are superimposed on the two PECs, dissociating to  $\text{C}(^3\text{P}_g) + \text{N}(^4\text{S}_u)$  and  $\text{C}(^3\text{P}_g) + \text{N}(^2\text{D}_u)$  atomic limits. Because at the CASSCF level the EV approach renders a "legitimate" procedure<sup>47</sup> for calculating one-electron molecular properties, and considering the extent of the reference configuration space (e.g., the number of configuration state functions for the AS (4+2,22) and (433) is 3596 and 6976, respectively), the closeness of the MCSCF and icMRCI EFG curves suggests credibility of the EV icMRCI EFG values. In the asymptotic region,  $q^{\text{N}}(R)$  tends to zero for the electronic GS, as it corresponds to spherical symmetry of the  $\text{N}(^4\text{S}_u)$  state, and to the values of  $-0.0932$  a.u. (icMRCI) and  $-0.0556$  a.u. (MCSCF) for the  $B^2\Sigma^+$  state (at  $R = 10$  bohr), which well comply with the atomic calculation on the  $\text{N}(^2\text{D}_u)$  state with the same AO

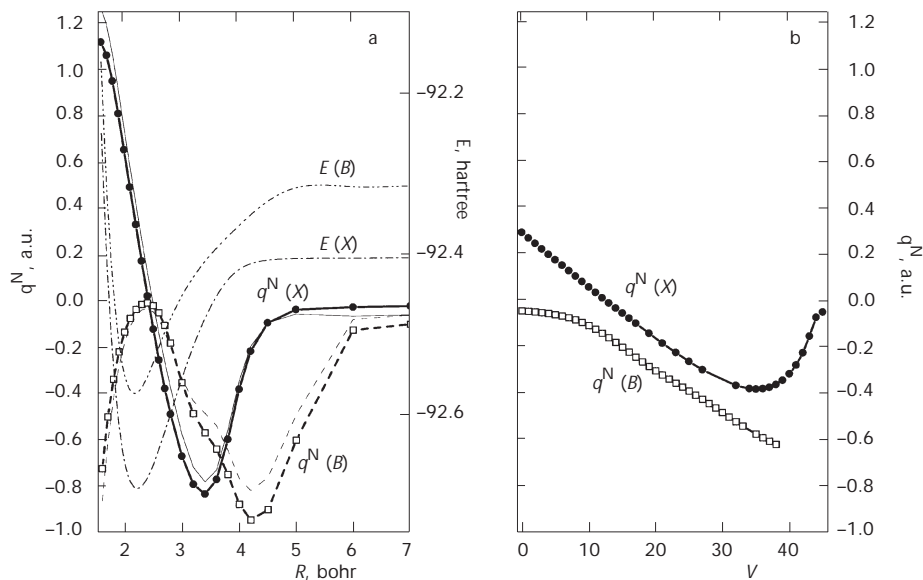


FIG. 1

Nitrogen EFGs in the CN  $X$  and  $B^2\Sigma^+$  electronic states as functions of a internuclear separation  $R$  and  $v$  vibration quantum number  $v$ , obtained with (2-S) CAS(4+2,22)SCF (thin) and icMRCI (thick and symbols) calculations, basis aCV5Z. The icMRCI potential energy functions (a) are represented by dash-dot curves

basis set, yielding the field gradients of  $-0.1156$  a.u. (icMRCI) and  $-0.1144$  a.u. (MCSCF). As N and C approach each other, the  $q^N(\mathbf{R})$  curves of both  ${}^2\Sigma^+$  species decrease until they reach minima lying below  $-0.8$  a.u. at about  $R$  equal to 4.2 and 3.4 bohr for the  $B$  and  $X$  states, respectively. Upon further approach of the atoms, both curves are steeply rising, and thus – from a qualitative view – testifying to an extensive reorganization of  $p_\pi$  and  $p_\sigma$  orbital electron occupancy<sup>23,51</sup> at N. In the region near the equilibrium distance  $R_e$ , the wave functions of the  $X$  and  $B$  states are dominated by the MO configurations  $[\dots(4\sigma)^2(5\sigma)^1(1\pi_x)^2(1\pi_y)^2]$  and  $[\dots(4\sigma)^1(5\sigma)^2(1\pi_x)^2(1\pi_y)^2]$ , respectively. While  $q^N(\mathbf{R})$  for the  $B$  state traverses a maximum before dropping again to low values, the EFG for the  $X$  state climbs steeply towards large (*i.e.* above 1 a.u.) positive values, indicating a massive excess of electrons in the nitrogen  $p_\sigma$  orbitals compared to the number of electrons in the  $p_\pi$  orbitals<sup>23,51</sup>. The small EFG values in the vicinity of the equilibrium geometries and the steep course of the  $q^N(\mathbf{R})$  curve for the  $X$  state lead to the assumption that the relative error in estimating the EFG value at  $R_e$  for the both  ${}^2\Sigma^+$  states of CN may be notable.

The dipole moment functions of  $R$ , together with the transition moment, are shown in Fig. 2a. The negative sign means that the positive end of  $\mu$  is

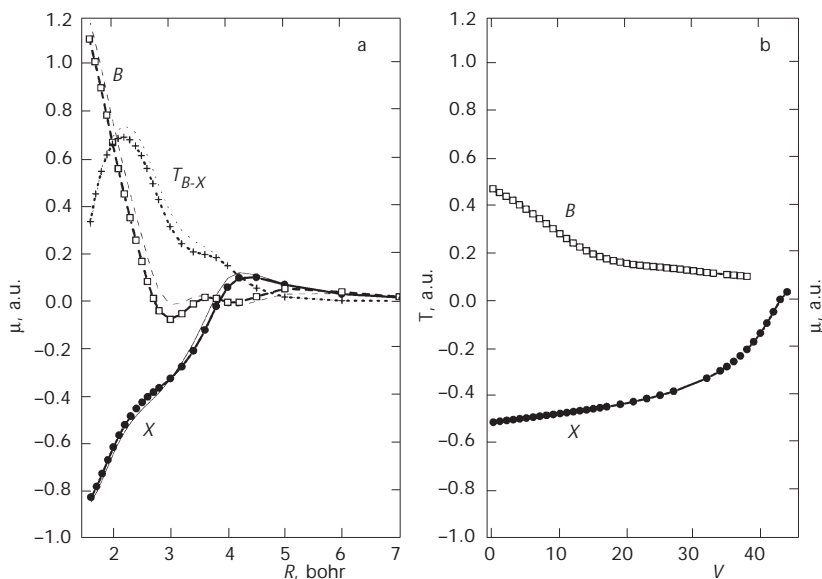


FIG. 2

Electric dipole moments (and transition moment  $T$ ) of the CN  $X$  and  $B^2\Sigma^+$  electronic states as functions of a internuclear separation  $R$  and b) vibration quantum number  $v$ , obtained with (2-S) CAS(4+2,22)SCF (thin) and icMRCI (thick and symbols) calculations, basis aCV5Z

at the carbon site. It is apparent from this figure that the dipole moments of the  $X$  and  $B$  states are of reverse orientation at small internuclear separations including  $R_e$ , equally oriented in the vicinity of  $R \cong 3$  bohr, and changing the direction of  $\mu$  for the  $X$  state from  $\text{C}^+\text{N}^-$  to  $\text{C}^-\text{N}^+$  at still larger  $R$ . The wavy shape exhibited by  $q^{\text{N}}(R)$  (Fig. 1a) and  $\mu(R)$  (Fig. 2a) for the  $B$  state, and the transition moment curve (Fig. 2a), starting at about  $R \cong 3$  bohr, may be attributed to robust changes in the wave function composition: For example, the electron configuration dominant at the equilibrium separation switches to prevalence of  $\{[\dots(4\sigma)^2(5\sigma)^1(1\pi_x)^1(2\pi_x)^1(1\pi_y)^2] + [\dots(4\sigma)^2(5\sigma)^1(1\pi_x)^2(1\pi_y)^1(2\pi_y)^1]\}$  at  $R \cong 3$  bohr.

The right-hand panels of Figs 1 and 2 present the EFGs at N and dipole moments of both  $^2\Sigma^+$  states as functions of the vibrational quantum number  $v$ . Note that both  $X$ -state quantities extend "linearity" for low lying values of  $v$  within a much wider range of vibrational quantum numbers compared to the quantities related to the  $B$  state. This situation bears on the type of numerical representation of the results in the form of fitting formulae, as they are displayed in Tables I through IV. The vibrationally averaged EFGs and dipole moments calculated at various levels of approximation are expressed by means of parameters  $b_i$  corresponding to fitting functions in the form of power series

$$f(v) = \sum_{i=0}^n b_i \left( v + \frac{1}{2} \right)^i, \quad (2)$$

using curve fits within the range  $0 \leq v \leq v_{\text{max}}$ .  $v_{\text{max}}$  was chosen equal to 15 (exceptionally 11, if convergence difficulties in obtaining the MRCI solution hampered acquisition of a sufficiently complete PEC) or 8, depending on whether properties pertinent to the  $X$  or  $B$  state were expressed.

The vibrational dependence of the field gradient at N and the  $^{14}\text{N}$  QCC,  $v = 0$ , for the  $X^2\Sigma^+$  state, calculated with several ASs and using three AO basis sets, is displayed in Table I. Since  $q^{\text{N}}(v)$  is almost linear in the above defined interval (e.g., with the (2-S) CASSCF(4+2,22)/icMRCI calculation using the aCV5Z basis set one obtains  $[0.3050, -0.0234]$ ,  $[0.3071, -0.0241, 5 \times 10^{-5}]$  and  $[0.3061, -0.0234, -7 \times 10^{-5}, 5 \times 10^{-6}]$ , where the numbers in brackets represent parameters  $b_i$  in linear, quadratic and cubic fitting functions, respectively), linear functions were used for fitting. This form complies with the Buckingham formula<sup>52</sup> in the linear dependence on  $(v + 1/2)$ . The latter approach, however, differs in that the vibrational averaging and fitting procedure are replaced by expressing the parameters in terms of spectroscopic

TABLE I  
Vibrational and basis set dependences of the  $^{14}\text{N}$  QCC in the  $X^2\Sigma^+$  state of CN as obtained by icMRCI calculations

AS	No. of states	aVQZ		aV5Z		aCV5Z				
		$q^N, \text{a.u.}^a$		$q^N, \text{a.u.}^a$		$q^N, \text{a.u.}^a$				
		$X_{v=0}^N$ MHz	$b_0$	$b_1$	$X_{v=0}^N$ MHz	$b_0$	$b_1$	$X_{v=0}^N$ MHz	$b_0$	$b_1$
422	1	1.629	0.3510	-0.0255	1.645	0.3541	-0.0255	1.593	0.3431	-0.0248
	2	1.315	0.2847	-0.0239	1.329	0.2876	-0.0239	1.305	0.2822	-0.0235
4+2,22	1	1.778	0.3823	-0.0258	1.819	0.3906	-0.0258	1.796 <sup>b</sup>	0.3855	-0.0253
	2	1.429	0.3085	-0.0240	1.460	0.3148	-0.0240	1.415 <sup>c</sup>	0.3050	-0.0234
522	1	1.699	0.3658	-0.0262	1.715	0.3692	-0.0261	1.661	0.3574	-0.0255
	1	1.867	0.4014	-0.0265	1.913	0.4106	-0.0266	-	-	-
5+2,22	2	1.402	0.3032	-0.0240	1.432	0.3091	-0.0239	-	-	-
433	1	1.498	0.3237	-0.0251	1.513	0.3268	-0.0251	1.466	0.3167	-0.0245
	2	1.294	0.2810 <sup>d</sup>	-0.0245	1.309 <sup>d</sup>	0.2839	-0.0246	1.285	0.2788 <sup>d</sup>	-0.0241
533	1	1.544	0.3353	-0.0256	-	-	-	-	-	-
	2	1.291	0.2809	-0.0242	-	-	-	-	-	-

<sup>a</sup> The linear fitting functions encompass values within the range  $0 \leq v \leq 15$  with the exception of cases denoted by <sup>d</sup>. <sup>b</sup> icMRCI+Q evaluation of the PEC leads to 1.779 MHz (with  $b_0 = 0.3821$ ,  $b_1 = -0.0254$  for  $q^N$  (a.u.)). <sup>c</sup> icMRCI+Q evaluation of the PEC leads to 1.411 MHz (with  $b_0 = 0.3043$ ,  $b_1 = -0.0236$  for  $q^N$  (a.u.)). <sup>d</sup> The linear fitting functions encompass values within the range  $0 \leq v \leq 11$ .



constants. For low-lying vibrational excitations in the electronic GSs of  $\text{CN}^+$  and  $\text{CN}^-$ , both ways of the EFG description gave remarkably similar results<sup>32</sup>; the same is expected with  $\text{CN}$ . As seen in Table I, the  $^{14}\text{N}$  QCC values in the electronic and vibrational GSs are only slightly sensitive to the choice of the basis set, but depend in a noticeable way on the active orbital space used in CASSCF/icMRCI calculations, and even more on whether the (1-S) or (2-S) approach is applied. A four-state-averaged CASSCF/icMRCI calculation, with equal weights for three  $^2\Sigma^+$  states and one component of the  $^2\Delta$  state, gave for the EFG very close results to the (2-S) calculation in the medium region of internuclear separations where appropriate convergence of the solution took place.

While the extension of the AS consisting of valence orbitals by  $\sigma$  orbitals, primarily by core molecular orbitals, gives rise to an increase in  $X_{v=0}^{\text{N}}$ , the extension by  $\pi$  orbitals leads to a decrease in  $X_{v=0}^{\text{N}}$ . Particularly noteworthy in Table I is the alteration of  $X_{v=0}^{\text{N}}$  due to the extension of the AS by 1s-like orbitals in all cases under consideration, allowing to approximately estimate the core correlation contribution to this quantity. These changes of the  $^{14}\text{N}$  QCC amount to about 8–13%, which is about 20 times more than analogously created variations of the  $^{14}\text{N}$  QCCs in the closed shell electronic ground states<sup>32</sup> of  $\text{CN}^+$  and  $\text{CN}^-$ .

State-averaging is an element of ambiguity in the CASSCF/icMRCI calculations and brings about a computational advantage in treating excited states<sup>19</sup>. Although it does affect the total energy unimportantly, as will be seen later on, state-averaging of the lowest two  $^2\Sigma^+$  states brings about a substantial decrease in  $X_{v=0}^{\text{N}}$  with respect to the (1-S) calculations, ranging from about 25% for the (5+2,22) AS to about 12–13% for the (433) AS. Within the types of computations defined in Table I, the values of  $X_{v=0}^{\text{N}}$  lie in the intervals (1.466,1.913) and (1.285,1.460) MHz, associated with (1-S) and (2-S) calculations, respectively. It is to be noticed in this table that the slopes (*i.e.*  $b_1$  parameters) of the  $v$ -dependences are also somewhat smaller for the (2-S) calculations than for the (1-S) ones.

Our estimates of the  $^{14}\text{N}$  QCCs obtained from the (2-S) CAS(433)SCF/icMRCI calculations (*e.g.*, with basis set aCV5Z, 1.285 MHz ( $v=0$ ) and 1.166 MHz ( $v=1$ )) compare well with the experimental findings for the magnitude of this quantity, 1.307 MHz ( $v=0$ ) and 1.263 MHz ( $v=1$ )<sup>5</sup>, and 1.275 MHz ( $v=0$ ) and 1.178 MHz ( $v=1$ )<sup>8</sup>. It appears, therefore, opportune to complement the vibrational dependence also by the rotational one, though at present no experimental counterpart exists. The EFG at N as a function of both vibrational ( $v$ ) and end-over-end rotational ( $N$ ) quantum numbers is displayed in Fig. 3, and expressed numerically by the fitting function

$$f(v, N) = \sum_{i=0}^3 a_i \left( v + \frac{1}{2} \right)^i + c_1 N(N+1) + c_2 N(N+1) \left( v + \frac{1}{2} \right), \quad (3)$$

where the parameters (in a.u.) assume the values  $\mathbf{a} = [0.28005, -2.4979 \times 10^{-2}, 1.324 \times 10^{-4}, -5.838 \times 10^{-6}]$  and  $\mathbf{c} = [-1.20317 \times 10^{-5}, -5.55 \times 10^{-8}]$ . It is seen that, within the range of fitted quantum numbers, the rotational excitation leads to a decrease in  $q^N$ , depending quadratically on  $N$ . Clearly, the rotational excitation is less significant than the vibrational one. For instance, the change of  $q^N$  with the excitations  $N = 10 \leftarrow N = 0$  and  $N = 50 \leftarrow N = 40$  in the  $v = 0$  state is predicted from our calculation to be 5 and 44% of the change in  $q^N$  accompanying the excitation  $v = 1, N = 0 \leftarrow v = 0, N = 0$ , respectively.

The vibrational dependence of the dipole moment of CN in its electronic GS, as a function of the AS, AO basis set and the CASSCF calculation approach (*i.e.*, (1-S) or (2-S)), is presented in Table II. One observes there that the calculation of  $\mu$  is also affected by these three factors as the field gradient, though the result is less sensitive to the AS and AO basis set used. For instance, the extension of the AS by 1s-like orbitals affects  $\mu$  much less than the EFG, and the alteration is comparable with that found<sup>32</sup> for the electronic ground states of  $\text{CN}^+$  and  $\text{CN}^-$ . The magnitude of  $\mu$  lies in the intervals  $\langle 1.388, 1.549 \rangle$  and  $\langle 1.287, 1.372 \rangle$  D, associated with (1-S) and (2-S) calculations, respectively. Thus, as in the case of the EFG values, the inter-

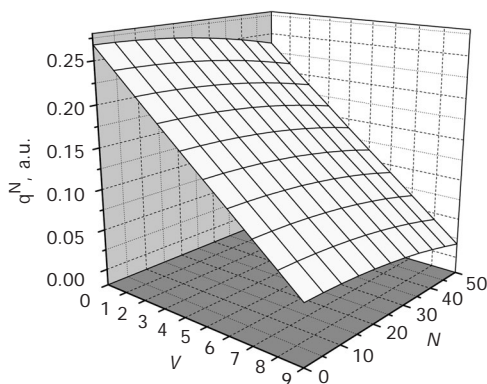


FIG. 3

Nitrogen EFG in the  $X^2\Sigma^+$  electronic state of CN as a function of vibration  $v$  and end-over-end rotation  $N$  quantum numbers, obtained with the (2-S) CAS(433)SCF/icMRCI calculation, basis aCV5Z

TABLE II

 Vibrational and basis set dependences of the electric dipole moment  $\mu$  of the  $\text{CN X}^2\Sigma^+$  state as obtained by icMRCI calculations

AS	No. of states	aVQZ			aV5Z			aCV5Z		
		$\mu(v=0)$ D	$b_0^a$	$b_1$	$\mu(v=0)$ D	$b_0^a$	$b_1$	$\mu(v=0)$ D	$b_0^a$	$b_1$
422	1	-1.435	-1.4418	0.0112	-1.439	-1.4457	0.0113	-1.440	-1.4460	0.0113
	2	-1.301	-1.3077	0.0089	-1.304	-1.3101	0.0089	-1.304	-1.3099	0.0089
4+2,22	1	-1.462	-1.4688	0.0118	-1.470	-1.4765	0.0119	-1.477 <sup>b</sup>	-1.4841	0.0122
	2	-1.308	-1.3141	0.0092	-1.311	-1.3171	0.0093	-1.302 <sup>c</sup>	-1.3087	0.0094
522	1	-1.494	-1.5009	0.0123	-1.499	-1.5054	0.0124	-1.499	-1.5058	0.0124
5+2,22	1	-1.538	-1.5449	0.0131	-1.549	-1.5559	0.0134	-	-	-
	2	-1.366	-1.3725	0.0100	-1.372	-1.3784	0.0102	-	-	-
433	1	-1.388	-1.3938	0.0104	-1.392	-1.3976	0.0105	-1.392	-1.3978	0.0105
	2	-1.287	-1.2913 <sup>d</sup>	0.0083	-1.289	-1.2935 <sup>d</sup>	0.0084	-1.289	-1.2933 <sup>d</sup>	0.0084
533	1	-1.437	-1.4446	0.0099	-	-	-	-	-	-
	2	-1.292	-1.2986	0.0090	-	-	-	-	-	-

<sup>a</sup> The linear fitting functions encompass values within the range  $0 \leq v \leq 15$  with the exception of cases denoted by <sup>d</sup>. <sup>b</sup> icMRCI+Q evaluation of the PEC leads to -1.475 D ( $b_0 = -1.4819$ ,  $b_1 = 0.0123$ ). <sup>c</sup> icMRCI+Q evaluation of the PEC leads to -1.302 D ( $b_0 = -1.3083$ ,  $b_1 = 0.0095$ ). <sup>d</sup> The linear fitting functions encompass values within the range  $0 \leq v \leq 11$ .

vals related to the type of CASSCF calculation do not overlap. The experimentally determined value<sup>53</sup> of  $1.45 \pm 0.08$  D lies within the range of the single-state calculations, being best reproduced by the (1-S) CAS(422)SCF/icMRCI calculation using the aCV5Z basis set, for which we, therefore, also give a fitted vibrational-rotational function in the form of Eq. (3), with the parameters (in D) taking on the values  $\mathbf{a} = [-1.4455, 1.1395 \times 10^{-2}, -8.41 \times 10^{-5}, 5.78 \times 10^{-6}]$  and  $\mathbf{c} = [8.1057 \times 10^{-6}, -5.36 \times 10^{-8}]$ .

The application of the EV approach to the calculation of both electric quantities,  $q^N$  and  $\mu$ , deserves a word of caution. In using a state-averaged CASSCF/icMRCI calculation with a less extensive basis set, Knowles *et al.*<sup>19</sup> found only insignificant differences between ED and EV calculations on dipole moments of the CN  $X^2\Sigma^+$ ,  $B^2\Sigma^+$  and  $^2\Pi$  states. Our EV and ED icMRCI estimates of the  $X$  state dipole moment function are compared graphically with the corresponding MCSCF values in Fig. 4. At  $R = 2.2$  bohr the magnitude of  $\mu$ ,  $|\mu| = 1.465$  D, calculated as EV, lies by 0.095 D higher than the ED value and evidently closer to experimental value. Interestingly, the EV values follow the MCSCF curve more closely than the ED values in the whole region of internuclear separations. Concerning the EFG computations, Cummins *et al.*<sup>26</sup> found for  $q^N$  in CN the largest non-Hellmann-Feynman corrections among all investigated nitrogen-containing compounds, and the largest differences between results produced by various quantum-chemical methods as well. Our test calculations with MOLCAS, for a limited number of ASs, the aVQZ basis and in a narrow range of inter-

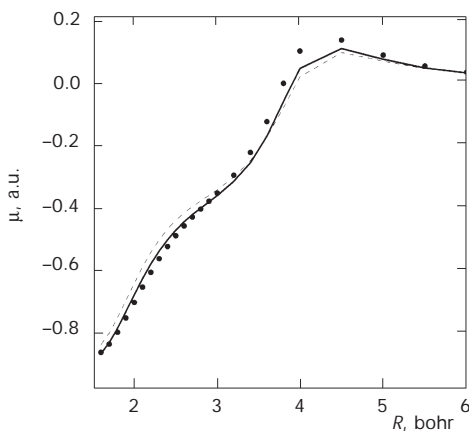


FIG. 4

Comparison of electric dipole moment curves  $\mu(R)$  of the CN  $X^2\Sigma^+$  state as calculated according to various formalisms: (1-S) CASSCF (solid circle), icMRCI EV (thick) and icMRCI ED (thin), AS (422), basis aVQZ

TABLE III  
 Vibrational and basis set dependences of the  $^{14}\text{N}$  QCC in the  $\text{B}^2\Sigma^+$  state of CN as obtained by icMRCI calculations

Basis	AS	422	4+2,22	5+2,22	433	533
aVQZ	$X_{v=0}^{\text{N}}$ , MHz	-0.135	-0.166	-0.200	-0.127	-0.115
	$q^{\text{N}}$ , a.u. <sup>a</sup>	$-2.659 \times 10^{-2}$	$-3.313 \times 10^{-2}$	$-4.024 \times 10^{-2}$	$-2.499 \times 10^{-2}$	$-2.240 \times 10^{-2}$
	$b_0$	$-2.759 \times 10^{-3}$	$-2.581 \times 10^{-3}$	$-2.491 \times 10^{-3}$	$-2.897 \times 10^{-3}$	$-2.802 \times 10^{-3}$
	$b_1$	$1.44 \times 10^{-5}$	$2.52 \times 10^{-5}$	$4.36 \times 10^{-5}$	$-8.40 \times 10^{-6}$	$1.77 \times 10^{-5}$
	$b_2$	$-4.57 \times 10^{-5}$	$-4.09 \times 10^{-5}$	$-4.31 \times 10^{-5}$	$-4.33 \times 10^{-5}$	$-4.89 \times 10^{-5}$
aV5Z	$X_{v=0}^{\text{N}}$ , MHz	-0.160	-0.197	-0.233	-0.152	
	$q^{\text{N}}$ , a.u. <sup>a</sup>	$-3.203 \times 10^{-2}$	$-3.981 \times 10^{-2}$	$-4.739 \times 10^{-2}$	$-3.035 \times 10^{-2}$	
	$b_0$	$-2.570 \times 10^{-3}$	$-2.327 \times 10^{-3}$	$-2.224 \times 10^{-3}$	$-2.695 \times 10^{-3}$	
	$b_1$	$2.78 \times 10^{-5}$	$2.99 \times 10^{-5}$	$4.74 \times 10^{-5}$	$2.70 \times 10^{-6}$	
	$b_2$	$-4.55 \times 10^{-5}$	$-4.00 \times 10^{-5}$	$-4.20 \times 10^{-5}$	$-4.30 \times 10^{-5}$	
aCV5Z	$X_{v=0}^{\text{N}}$ , MHz	-0.200	-0.212	-	-0.191	
	$q^{\text{N}}$ , a.u. <sup>a</sup>	$-4.047 \times 10^{-2}$	$-4.300 \times 10^{-2}$		$-3.863 \times 10^{-2}$	
	$b_0$	$-2.171 \times 10^{-3}$	$-2.198 \times 10^{-3}$		$-2.277 \times 10^{-3}$	
	$b_1$	$3.46 \times 10^{-5}$	$2.99 \times 10^{-5}$		$7.20 \times 10^{-6}$	
	$b_2$	$-4.46 \times 10^{-5}$	$-3.86 \times 10^{-5}$		$-4.21 \times 10^{-5}$	

<sup>a</sup> The linear fitting functions encompass values within the range  $0 \leq v \leq 8$ .

nuclear distances around  $R_e$ , indicate that the non-Hellmann–Feynman corrections are smaller than the alterations in the icMRCI solutions arising from choices of different ASs and types of averaging the CASSCF solution. Particularly at  $R = 2.2$  bohr, *e.g.*, the (1-S) CASSCF(422)/icMRCI EV calculation yields  $q^N$  equal to 0.3887 a.u., and the CASSCF/direct MRCI (MOLCAS) calculations give 0.3668 and 0.3522 a.u., depending on whether the EV or ED approach is applied.

Analogous data to those presented in Tables I and II, obtained from the (2-S) CASSCF/MRCI calculations for the  $B^2\Sigma^+$  state are collected in Tables III and IV. The  $^{14}\text{N}$  QCC and the dipole moment in the vibrational ground state acquire values in the intervals  $\langle -0.115, -0.233 \rangle$  MHz (Table III) and  $\langle 1.110, 1.202 \rangle$  D (Table IV), respectively. The former quantity can only be compared with the NQCC lying in the interval  $-5 \pm 5$  MHz experimentally determined<sup>6,7</sup> almost forty years ago. Our theoretical values for  $\mu(v=0)$  well encompass the experimental estimate  $1.15 \pm 0.08$  D of Thomson and Dalby<sup>53</sup>.

In order to add further support to the overall quantitative correctness of the correlated wave functions used in our calculations, the total energies at

TABLE IV  
Vibrational and basis set dependences of the electric dipole moment  $\mu$  of the CN  $B^2\Sigma^+$  state as obtained by icMRCI calculations

Basis	AS	422	4+2,22	5+2,22	433	533
aVQZ	$\mu(v=0)$ , D <sup>a</sup>	1.139	1.180	1.187	1.114	1.110
	$b_0$	1.1583	1.1994	1.2068	1.1339	1.1295
	$b_1$	-0.0386	-0.0377	-0.0384	-0.0399	-0.0387
	$b_2$	-0.0010	-0.0010	-0.0010	-0.0008	-0.0009
aV5Z	$\mu(v=0)$ , D <sup>a</sup>	1.145	1.194	1.202	1.120	-
	$b_0$	1.1642	1.2130	1.2218	1.1396	
	$b_1$	-0.0386	-0.0379	-0.0386	-0.0399	
	$b_2$	-0.0010	-0.0010	-0.0010	-0.0008	
aCV5Z	$\mu(v=0)$ , D <sup>a</sup>	1.145	1.200	-	1.120	-
	$b_0$	1.1645	1.2190		1.1398	
	$b_1$	-0.0385	-0.0376		-0.0399	
	$b_2$	-0.0010	-0.0010		-0.0008	

<sup>a</sup> The linear fitting functions encompass values within the range  $0 \leq v \leq 8$ .

TABLE V  
Total energies and spectroscopic constants of the  $^{12}\text{C}^{14}\text{N } X^2\Sigma^+$  electronic state calculated with icMRCI, other methods and obtained by experiment

AS or method	NS <sup>a</sup>	Basis set	$R_e$ , Å	$E_e^b$ hartree	$D_e^c$ eV	$\omega_e$ cm <sup>-1</sup>	$\omega_e x_e$ cm <sup>-1</sup>	$B_e$ cm <sup>-1</sup>	$\alpha_e$ cm <sup>-1</sup>	
422	1	aVQZ	1.1759	0.583019	7.7072	2056.9	13.00	1.886	0.0172	
	2	aVQZ	1.1764	0.582938	7.7112	2055.8	13.02	1.885	0.0171	
	1	aV5Z	1.1749	0.586810	7.7293	2058.9	13.03	1.890	0.0173	
	2	aV5Z	1.1754	0.586730	7.7333	2057.9	13.04	1.888	0.0171	
	1	aCV5Z	1.1747	0.587438	7.7331	2059.6	13.02	1.891	0.0173	
	2	aCV5Z	1.1752	0.587367	7.7374	2058.7	13.06	1.888	0.0171	
	1 <sup>d</sup>	aug-cc-pV5Z	1.1748	–	7.763	2061	–	–	–	
	(+Q) <sup>e</sup>	1 <sup>d</sup> aug-cc-pV5Z	1.1758	–	7.730	2057	–	–	–	
4+2,22 <sup>f</sup>	1	aVQZ	1.1728	0.637536	7.8200	2071.4	13.06	1.897	0.0171	
	2	aVQZ	1.1734	0.637499	7.8260	2069.9	12.93	1.895	0.0170	
	1	aV5Z	1.1712	0.652140	7.8403	2071.5	12.92	1.902	0.0173	
	1	aug-cc-pV5Z <sup>g</sup>	1.1706	0.655066	7.8942	2079.7	13.06	1.903	0.0172	
	(+Q) <sup>e</sup>	1	aug-cc-pV5Z <sup>g</sup>	1.1716	0.670320	7.8568	2073.4	13.22	1.900	0.0174
	2	aV5Z	1.1719	0.652077	7.8460	2070.4	12.92	1.899	0.0172	
	2	aug-cc-pV5Z <sup>g</sup>	1.1713	0.654993	<sup>h</sup>	2078.5	13.01	1.901	0.0172	
	(+Q) <sup>e</sup>	2	aug-cc-pV5Z <sup>g</sup>	1.1714	0.671123	<sup>h</sup>	2074.8	13.10	1.900	0.0171
	1	aCV5Z	1.1716	0.694262	7.8062	2071.8	13.03	1.901	0.0173	
	2	aCV5Z	1.1723	0.694142	7.8108	2070.4	13.01	1.898	0.0171	
522	1	aVQZ	1.1756	0.584909	7.7126	2057.4	13.10	1.887	0.0171	
	2	aVQZ	1.1760	0.585019	<sup>h</sup>	2056.8	13.04	1.886	0.0170	
	1	aV5Z	1.1746	0.588726	7.7355	2059.3	13.05	1.891	0.0173	
	2	aV5Z	1.1751	0.588838	<sup>h</sup>	2058.4	12.95	1.889	0.0172	
	1	aCV5Z	1.1744	0.589363	7.7399	2059.9	13.03	1.891	0.0173	
	2	aCV5Z	1.1744	0.589363	7.7399	2059.9	13.03	1.891	0.0173	
5+2,22 <sup>f</sup>	1	aVQZ	1.1724	0.639732	7.8345	2071.7	12.98	1.898	0.0173	
	2	aVQZ	1.1729	0.639957	7.8473	2071.4	12.97	1.896	0.0170	
	1	aV5Z	1.1708	0.654417	7.8562	2072.3	12.93	1.903	0.0174	
	2	aV5Z	1.1714	0.654630	7.8681	2071.4	12.80	1.901	0.0173	
	1	aCV5Z	1.1747	0.590419	7.7305	2057.6	13.10	1.890	0.0174	
433	1	aVQZ	1.1758	0.585983	7.7039	2055.0	13.12	1.887	0.0174	
	2	aVQZ	1.1758	0.585850	7.8276	2054.9	13.26	1.886	0.0174	
	1	aV5Z	1.1749	0.589794	7.7264	2057.0	13.13	1.890	0.0174	
	2	aV5Z	1.1749	0.589665	7.8495	2057.5	13.39	1.889	0.0176	
	1	aCV5Z	1.1747	0.590419	7.7305	2057.6	13.10	1.890	0.0174	
	2	aCV5Z	1.1747	0.590302	7.8541	2057.3	13.21	1.889	0.0174	

TABLE V  
(Continued)

AS or method	NS <sup>a</sup>	Basis set	$R_e$ , Å	$E_e^b$ hartree	$D_e^c$ eV	$\omega_e$ cm <sup>-1</sup>	$\omega_e x_e$ cm <sup>-1</sup>	$B_e$ cm <sup>-1</sup>	$\alpha_e$ cm <sup>-1</sup>
533	1	aVQZ	1.1755	0.587934	7.7176	2060.5	13.86	1.889	0.0177
	2	aVQZ	1.1759	0.587860	7.7471	2058.0	13.12	1.887	0.0174
422 <sup>i</sup>	4	vD	1.178	0.573089	7.54	2048	13.1	1.879	0.0173
CCSD(T) <sup>j</sup>		aug-cc-pVQZ	1.1750	0.593672	–	2063.7	12.98	1.890	0.0172
CCSD(T) <sup>j</sup>		aug-cc-pV5Z	1.1739	0.600004	–	2067.7	12.93	1.893	0.0172
CCSD(T) <sup>j</sup>		aug-MTcc	1.1716	0.693051	–	2070.9	13.13	1.900	0.0174
CCSDT <sup>k</sup>		aug-cc-pVQZ	1.1739	0.594024	7.6408	2082	–	–	–
RMR CCSD <sup>l</sup>		cc-pVTZ	1.1736	0.553979	–	2081	13.6	1.892	0.0174
Expt <sup>m,n</sup>			1.1718 <sub>2</sub>	–	7.888	2068.59	13.087	1.900	0.0174
					7.866 <sup>o</sup>				
					7.901 <sup>p</sup>				
					7.723 <sup>q</sup>				

<sup>a</sup> No. of states in state-averaged calculations. <sup>b</sup> The total energy is reported as  $-(E + 92)$ . <sup>c</sup>  $D_e$  calculated within the supermolecule approach. <sup>d</sup> Ref.<sup>14</sup>. <sup>e</sup> PECs are calculated using the multireference analog of the Davidson correction. <sup>f</sup> Core orbitals included in the AS. <sup>g</sup> aug-cc-pV5Z +  $s_{\text{diff}}(\text{C})$  +  $s_{\text{diff}}(\text{N})$  basis set, cf. text. <sup>h</sup> No convergence at large  $R$ . <sup>i</sup> Ref.<sup>19</sup>, (13s8p3d2f)/[8531] van Duijneveldt basis set. <sup>j</sup> Ref.<sup>20</sup>. <sup>k</sup> Ref.<sup>16</sup>. <sup>l</sup> Ref.<sup>54</sup>. <sup>m</sup> Ref.<sup>55</sup>. <sup>n</sup> ZPE has been calculated as  $\omega_e/2 - \omega_e x_e/4$ , and added to  $D_0$ . <sup>o</sup> Ref.<sup>56</sup>. <sup>p</sup> Ref.<sup>57</sup>. <sup>q</sup> Cited in ref.<sup>16</sup>

$R_e$  and the spectroscopic constants derived from the PECs are collected in Tables V and VI, and compared with the available experimental and theoretical data. It appears from Table V that the energy and geometry parameters of the  $X^2\Sigma^+$  state are only slightly dependent on the basis set, and in most cases even less dependent on whether the (1-S) or (2-S) approach is applied, which is in contrast with the outcome of electric property calculations presented in Tables I through IV. Table V also shows, e.g., that for  $R_e$ ,  $D_e$  and  $\omega_e$  our icMRCI results, based on three choices of AO basis sets, two kinds of state-averaged CASSCF solutions and several active spaces, lie within intervals  $\langle 1.1708, 1.1764 \rangle$  bohr,  $\langle 7.7039, 7.8681 \rangle$  eV and  $\langle 2054.9, 2072.3 \rangle$  cm<sup>-1</sup>, respectively. Further, the outcome based on calculations with core orbitals included in the AS and using the aCV5Z basis is in excellent agreement with experiment and other high-level computations. For the  $B^2\Sigma^+$  state, the energy parameters and spectroscopic constants in Table VI show much the same sensitiveness with the basis set and active space as the  $X$  state. The  $R_e$ ,  $D_e$  and  $\omega_e$  values, for instance, lie within intervals  $\langle 1.1503, 1.1554 \rangle$  bohr,  $\langle 6.9255, 7.0463 \rangle$  eV and  $\langle 2152.2, 2176.7 \rangle$  cm<sup>-1</sup>, re-



spectively, *i.e.*, again well in accord with the experimental data. The good description of the  $X$  and  $B^2\Sigma^+$  states in terms of spectroscopic constants seems to indicate a balanced treatment of both states.

In using the complete aug-cc-pV5Z basis set + additional diffuse functions in the calculations, the effects of the inclusion of  $h$  functions (*cf.* Tables V and VI) and the Davidson correction (*cf.* Tables I through VI) on the results have been found insignificant, the latter evidence suggesting hardly observable size-consistency violation<sup>58</sup> by the icMRCI-type wave functions. The addition of  $h$  functions alters, *e.g.* at  $R = 2.2$  bohr, the dipole moment value of CN in the  $X$  state by about 0.2%, and also extension of the AO basis set by “tight” functions<sup>59</sup> has only negligible effect on the calculated electric properties.

TABLE VI  
Total energies and spectroscopic constants of the  $^{12}\text{C}^{14}\text{N}$   $B^2\Sigma^+$  electronic state calculated with icMRCI, other methods and obtained by experiment

AS	Basis set	$R_e$ , Å	$E_e^a$ hartree	$D_e^b$ eV	$T_e$ eV	$\omega_e$ cm <sup>-1</sup>	$\omega_e x_e$ cm <sup>-1</sup>	$B_e$ cm <sup>-1</sup>	$\alpha_e$ cm <sup>-1</sup>
422	aVQZ	1.1549	0.464341	6.9255	3.2272	2161.3	21.93	1.959	0.021
	aV5Z	1.1539	0.468235	6.9427	3.2244	2165.0	21.77	1.962	0.021
	aCV5Z	1.1538	0.468860	6.9449	3.2247	2162.0	20.79	1.961	0.020
4 + 2,22 <sup>c</sup>	aVQZ	1.1521	0.519639	6.9357	3.2071	2176.7	21.00	1.968	0.020
	aV5Z	1.1505	0.534425	6.9548	3.2015	2171.6	18.65	1.970	0.019
	aug-cc-pV5Z <sup>d</sup>	1.1501	0.537329	<sup>e</sup>	3.2018	2185.8	20.17	1.973	0.020
	(+Q) <sup>f</sup> aug-cc-pV5Z <sup>d</sup>	1.1509	0.554476	<sup>e</sup>	3.1741	2177.9	20.25	1.970	0.020
	aCV5Z	1.1509	0.576091	7.0440	3.2123	2171.4	18.81	1.969	0.019
522	aVQZ	1.1548	0.466205	<sup>e</sup>	3.2331	2161.7	21.91	1.959	0.021
	aV5Z	1.1538	0.470117	<sup>e</sup>	3.2306	2161.6	20.83	1.961	0.020
5 + 2,22 <sup>c</sup>	aVQZ	1.1519	0.521779	7.0267	3.2158	2171.3	19.39	1.966	0.019
	aV5Z	1.1503	0.536632	7.0463	3.2109	2173.0	18.71	1.971	0.019
433	aVQZ	1.1554	0.467315	<sup>e</sup>	3.2255	2152.2	23.44	1.960	0.023
	aV5Z	1.1544	0.471226	<sup>e</sup>	3.2229	2155.8	23.28	1.963	0.023
	aCV5Z	1.1542	0.471850	<sup>e</sup>	3.2232	2156.7	23.25	1.964	0.023
533	aVQZ	1.1546	0.469166	<sup>e</sup>	3.2298	2160.5	22.13	1.960	0.022
422	vD <sup>g</sup>	1.156	0.454328	6.80	3.2319	2142	20.1	1.950	0.021
Expt <sup>h</sup>		1.150		6.97 <sup>i</sup>	3.1928	2163.9	20.2	1.973	0.023

<sup>a</sup> The total energy is reported as  $-(E + 92)$ . <sup>b</sup>  $D_e$  calculated within the supermolecule approach.

<sup>c</sup> Core orbitals included in the AS. <sup>d</sup> aug-cc-pV5Z +  $s_{\text{diff}}(\text{C})$  +  $s_{\text{diff}}(\text{N})$  basis set, *cf.* text. <sup>e</sup> No convergence at large  $R$ . <sup>f</sup> PECs are calculated using the multireference analog of the Davidson correction. <sup>g</sup> Ref.<sup>19</sup>, (13s8p3d2f)/[8531] van Duijneveldt basis set. <sup>h</sup> Ref.<sup>55</sup>. <sup>i</sup> Cited in ref.<sup>19</sup>

## CONCLUSIONS

The purpose of this work was to determine the  $^{14}\text{N}$  QCCs in the  $X^2\Sigma^+$  and  $B^2\Sigma^+$  electronic states of CN, and the rovibrational dependences of these constants. The electronic structure calculations employed augmented correlation-consistent basis sets and the correlation energy was taken into account by the internally contracted multireference configuration procedure of Werner and Knowles. The relativistic effects were assumed to be small and have not been taken into account. The good overall quality of the wave functions was confirmed by comparing electric dipole moments and potential energy curves, represented in terms of derived spectroscopic constants, with experimental and high-level theoretical data. The wave functions were used for calculating expectation values of the principal component  $q^{\text{N}}$  of the electric field gradient at the nitrogen nucleus, which were subsequently applied to the estimation of the effect of rovibrational excitation on the quadrupole hyperfine patterns. The calculated value of  $q^{\text{N}}$  is sensitive to the choice of active orbital space and state averaging in the CASSCF procedure. Estimates of the core correlation contributions appear to be more important in calculating  $q^{\text{N}}$  in CN than in its related ions  $\text{CN}^+$  and  $\text{CN}^-$ . An important qualitative feature of the  $^{14}\text{N}$  QCC in the  $X^2\Sigma^+$  state is that it declines linearly in its magnitude with vibrational excitation until changing sign at about  $v \approx 12$ . The calculated values of the  $^{14}\text{N}$  QCC for two vibrational states, obtained from the (2-S) CAS(433)SCF/icMRCI calculation using the basis set aCV5Z, are in good accord with experimental findings<sup>5,8</sup>. Therefore, at this level of approximation,  $q^{\text{N}}$  was expressed in the form of a fitting function of both vibrational ( $v$ ) and end-over-end rotational ( $N$ ) quantum numbers. The appropriateness of the expectation value approach to the EFG and dipole moment calculations was discussed in the light of the results obtained with the energy derivative method.

*This work was supported by the Grant Agency of the Czech Republic (grant No. 203/01/1274). The study is a part of the long-term Research Plan of the Faculty of Science No. MSM 113100001. The time allocation in the Czech Academic Supercomputer Centre is greatly acknowledged.*

## REFERENCES

1. Combi M. R.: *Astrophys. J.* **1980**, *241*, 830.
2. Wyckoff S., Kleine M., Peterson B. A., Wehinger P. A., Ziurys L. M.: *Astrophys. J.* **2000**, *535*, 991.
3. Jefferts K. B., Penzias A. A., Wilson R. W.: *Astrophys. J.* **1970**, *161*, L87.
4. Penzias A. A., Wilson R. W., Jefferts K. B.: *Phys. Rev. Lett.* **1974**, *32*, 701.

5. Dixon T. A., Woods R. C.: *J. Chem. Phys.* **1977**, *67*, 3956.
6. Evenson K. M., Dunn J. L., Broida H. P.: *Phys. Rev.* **1964**, *136*, A1566.
7. Radford H. E.: *Phys. Rev.* **1964**, *136*, A1571.
8. Klisch E., Klaus T., Belov S. P., Winnewisser G., Herbst E.: *Astron. Astrophys.* **1995**, *304*, L5.
9. Li X., Paldus J.: *Mol. Phys.* **1998**, *94*, 41.
10. Peris G., Rajadell F., Li X., Planelles J., Paldus J.: *Mol. Phys.* **1998**, *94*, 235.
11. Li X., Paldus J.: *Mol. Phys.* **2002**, *98*, 1185.
12. Neogrady P., Medved' M., ˇCernusak I., Urban M.: *Mol. Phys.* **2002**, *100*, 541.
13. Bauschlicher C. W., Jr., Langhoff S. R., Taylor P. R.: *Astrophys. J.* **1988**, *332*, 531.
14. Pradhan A. D., Partridge H., Bauschlicher C. W., Jr.: *J. Chem. Phys.* **1994**, *101*, 3857.
15. Feller D., Sordo J. A.: *J. Chem. Phys.* **2000**, *113*, 485.
16. Sordo J. A.: *J. Chem. Phys.* **2001**, *114*, 1974.
17. Green S.: *J. Chem. Phys.* **1972**, *57*, 4694.
18. Urban M., Neogrady P., Raab J., Diercks G. H. F.: *Collect. Czech. Chem. Commun.* **1998**, *63*, 1409.
19. Knowles P. J., Werner H.-J., Hay P. J., Cartwright D. C.: *J. Chem. Phys.* **1988**, *89*, 7334.
20. Lee T. J., Dateo C. E.: *Spectrochim. Acta, Part A* **1999**, *55*, 739.
21. Fernandez B., Jorgensen P., Simons J.: *J. Chem. Phys.* **1993**, *98*, 7012.
22. Sugden T. M., Kenney C. N.: *Microwave Spectroscopy of Gases*. Van Nostrand, London 1965.
23. Townes C. H., Dailey B. P.: *J. Chem. Phys.* **1949**, *17*, 782.
24. Gordy W.: *Discuss. Faraday Soc.* **1955**, *19*, 14.
25. Purcell K. F.: *J. Chem. Phys.* **1968**, *48*, 5735.
26. Cummins P. L., Bacskay G. B., Hush N. S., Ahlrichs R.: *J. Chem. Phys.* **1987**, *86*, 6908.
27. Bacis R., Broyer M., Churassy S., Verges J., Vigue J.: *J. Chem. Phys.* **1980**, *73*, 2641.
28. Ubachs W., Meyer G., ter Meulen J. J., Dymanus A.: *J. Mol. Spectrosc.* **1986**, *115*, 88.
29. Durand A., Loison J. C., Bazalgette G., Gangler E., Dalby F. W., Vigue J.: *Chem. Phys.* **1994**, *181*, 209.
30. Fiser J., Vojtık J.: *Chem. Phys.* **1994**, *182*, 217.
31. Vojtık J., Fiser J.: *Chem. Phys.* **1997**, *218*, 13.
32. Polak R., Fiser J.: *Spectrochim. Acta, Part A* **2002**, *58*, 2029.
33. Paidarova I., Vojtık J., ˇCespiva L., ˇSavrda J., ˇSpirko V.: *Int. J. Quantum Chem.* **1990**, *38*, 283.
34. Vojtık J., ˇCespiva L., Paidarova I., ˇSavrda J.: *J. Mol. Struct. (THEOCHEM)* **1991**, *227*, 111.
35. Werner H.-J., Knowles P. J.: *J. Chem. Phys.* **1988**, *89*, 5803.
36. Knowles P. J., Werner H.-J.: *Chem. Phys. Lett.* **1988**, *145*, 514.
37. Werner H.-J., Knowles P. J., with contributions from Amos R. D., Bernhardsson A., Berning A., Celani P., Cooper D. L., Deegan M. J. O., Dobbyn A. J., Eckert F., Hampel C., Hetzer G., Korona T., Lindh R., Lloyd A. W., McNicholas S. J., Manby F. R., Meyer W., Mura M. E., Nicklass A., Palmieri P., Pitzer R., Rauhut G., Schutz M., Stoll H., Stone A. J., Tarroni R., Thorsteinsson T.: *MOLPRO 2000.1*. Universitat Stuttgart and University of Birmingham 2000.
38. Knowles P. J., Werner H.-J.: *Chem. Phys. Lett.* **1985**, *115*, 259.
39. Werner H.-J., Knowles P. J.: *J. Chem. Phys.* **1985**, *82*, 5053.
40. Kendall R. A., Dunning T. H., Jr., Harrison R. J.: *J. Chem. Phys.* **1992**, *96*, 6796.
41. Woon D. E., Dunning T. H., Jr.: *J. Chem. Phys.* **1994**, *100*, 2975.

42. Woon D. E., Dunning T. H., Jr.: *J. Chem. Phys.* **1995**, *103*, 4572.
43. Andersson K., Blomberg M. R. A., Fülscher M. P., Karlström G., Lindh R., Malmqvist P.-Å., Neogrady P., Olsen J., Roos B. O., Sadlej A. J., Schütz M., Seijo L., Serrano-Andrés L., Siegbahn P. E. M., Widmark P.-O.: *MOLCAS-4*. Lund University, Lund 1997.
44. Langhoff S. R., Davidson E. R.: *Int. J. Quantum Chem.* **1974**, *8*, 61.
45. Blomberg M. R. A., Siegbahn P. E. M.: *J. Chem. Phys.* **1983**, *78*, 5682.
46. Cohen H. D., Roothaan C. C. J.: *J. Chem. Phys.* **1965**, *43*, S34.
47. Diercksen G. H. F., Roos B. O., Sadlej A. J.: *Chem. Phys.* **1981**, *59*, 29.
48. Cooley J. W.: *Math. Comput.* **1961**, *15*, 363.
49. deBoor C.: *A Practical Guide to Splines*. Springer, Berlin 1978.
50. Tokman M., Sundholm D., Pyykkö P., Olsen J.: *Chem. Phys. Lett.* **1997**, *265*, 60.
51. Polák R., Fišer J.: *J. Mol. Struct. (THEOCHEM)* **2002**, *584*, 69.
52. Buckingham A. D.: *J. Chem. Phys.* **1962**, *36*, 3096.
53. Thomson R., Dalby F. W.: *Can. J. Phys.* **1968**, *46*, 2815.
54. Li X., Paldus J.: *Mol. Phys.* **2000**, *98*, 1185.
55. Huber K. P., Herzberg G.: *Molecular Spectra and Molecular Structure*, Vol. 4. Van Nostrand Reinhold, New York 1979.
56. Huang Y., Barts S. A., Halpern J. B.: *J. Phys. Chem.* **1992**, *96*, 425.
57. Costes M., Naulin C., Dorthe G.: *Astron. Astrophys.* **1990**, *232*, 270.
58. Diercksen G. H. F., Kraemer W. P., Sadlej A. J.: *Chem. Phys. Lett.* **1981**, *82*, 117.
59. Olsen L., Christiansen O., Hemmingsen L., Sauer S. P. A., Mikkelsen K. V.: *J. Chem. Phys.* **2002**, *116*, 1424.